Physicochem. Probl. Miner. Process., 62(5), 2026, 236748 | Physicochemical Problems of Mineral Processing

http://www.journalssystem.com/ppmp | ISSN 1643-1049

Controlling the second-stage separation density in a gravity fed three product dense medium cyclone

Yusuf Enes Pural, Mustafa Özer, Fırat Burat, Feridun Boylu

Istanbul Technical University, Faculty of Mines, Mineral Processing Engineering Department, 34469 Maslak, Istanbul, Turkey

Corresponding author: pural@itu.edu.tr (Yusuf Pural)

Abstract: A three-product dense medium cyclone produces clean coal, middlings, and reject from a single medium circuit by joining a cylindrical primary separator of the LARCODEM type to a conical dense medium cyclone fed by the primary underflow. Although the operator sets only one circulating medium density, a second and higher separation density forms on its own in the secondary cyclone, because the primary unit sends coarser magnetite to its underflow and finer magnetite to its overflow. This secondary density has long been treated as fixed and beyond the operator's control. This work tested whether it can be adjusted intentionally. A pilot gravity fed unit was run under eighteen conditions set by a Taguchi L18 orthogonal array in five variables: the primary feed pipe immersion depth, the primary vortex finder depth, the secondary vortex finder depth, the feed pressure and the medium density. Partition curves were measured with plastic density tracers of three sizes, and the cut point, the probable error, the medium stability, and the medium split were obtained for both stages. Second-order models linked the geometry and the operating conditions to the secondary responses. The secondary density shift and the secondary medium stability were described with coefficients of determination of about 0.63 to 0.91. The primary feed pipe immersion depth was the main control variable, with feed pressure and secondary vortex finder depth as additional levers.

***Keywords*:** three-product dense medium cyclone, separation density, density tracer, response surface method, coal preparation

1. Introduction

Dense medium cyclones are the main equipment for washing coarse and intermediate-sized coal. The strong centrifugal field inside the cyclone provides fast, sharp density separation (He and Laskowski, 1995; Collins et al., 1983). The result is read from the Tromp partition curve, which gives the fraction of feed of a given density that reports to a product. Two numbers describe the curve: the cut point d_{50}, which is the density that splits equally between the two products, and the probable error E_p, which measures the spread of the curve. A small E_p means a sharp separation with few misplaced particles (King and Juckes, 1984; Wills and Finch, 2016).

The three-product dense medium cyclone was introduced to treat a wide size range in a single step and so shorten the conventional washing circuit. It places a cylindrical heavy medium vessel of the LARCODEM type ahead of a conical dense medium cyclone, with the second unit fed by the first unit's underflow (Shah, 1992). One circulating medium then yields clean coal, middlings, and reject together, which cuts both the number of units and the magnetite inventory compared with a circuit of separate stages (Jacobs and de Korte, 2013; Xia et al., 2013).

The feature that sets the three-product cyclone apart from a simple cascade of two units is the rise of the separation density in the second stage. The centrifugal field of the LARCODEM sends the coarser magnetite to the primary underflow and the finer magnetite to the primary overflow, so the medium that reaches the secondary cyclone is richer in fine magnetite and carries a higher apparent density than the medium that is pumped in. A second and higher cut point therefore forms in the secondary stage without any action by the operator (Shah, 1992; Pural et al., 2023). The size of the magnetite and the feed

DOI: 10.37190/ppmp/236748

pressure both affect how strong this density rise becomes (Davis and Napier-Munn, 1987; Fourie et al., 1980; O'Brien et al., 2014).

Several variables are known to shape the performance of any dense medium cyclone: the circulating medium density, the feed pressure, the vortex finder and spigot sizes, and the magnetite particle size (Luttrell et al., 2005; Napier-Munn, 1990). Feed pressure plays two opposite roles at once, because a higher pressure raises the centrifugal force, which sharpens the separation, but it also drives magnetite segregation, which can unsettle the cut point (Davis and Napier-Munn, 1987). The medium stability, taken as the density difference between the underflow and the overflow, should stay within about 0.1 to 0.4 g/cm^3; outside this range, the near-density material is held inside the cyclone and then leaves in a surge, which distorts the partition curve (Collins et al., 1983; Luttrell et al., 2005; Bosman, 2014). The split of medium to the overflow should also stay above two-thirds, so that the vortex is not overloaded (He and Laskowski, 1995).

Although the three-product cyclone is widely used, its secondary separation density has remained hard to set intentionally. Jacobs and de Korte (2013) suggested that orifice geometry could shift the secondary cut point but provided no measured evidence, and the simulation study by Pural et al. (2023) reproduced product yields without addressing how secondary density is controlled. No earlier work had used a designed experiment to separate the effect of each geometric and operating variable on the secondary cut point. The present study fills this gap. An 18-run Taguchi L18 orthogonal array (Taguchi, 1986) was applied to a gravity-fed pilot unit to answer two questions: whether the secondary separation density can be set on purpose through accessible variables, and which variables are the main levers.

2. Materials and methods

2.1. Pilot cyclone and medium

The tests used a gravity-fed three-product dense medium cyclone, modified for this work by KARBOMET Ltd. It joins a LARCODEM type cylindrical primary separator (length 91 cm, diameter 21 cm, feed pipe 30 cm) to a conical dense medium cyclone as the secondary stage (length 48 cm, diameter 23 cm). Fig. 1 shows the unit and names the adjustable geometric variables and the product streams. The circulating medium was prepared by mixing magnetite powder (45% passing 45 µm) with water, and its density was set and verified by weighing 1-liter samples. During each test, medium samples were drawn from four points, namely the primary overflow, the secondary cyclone feed, the secondary overflow that carries the middlings, and the secondary underflow that carries the reject, so that the stream densities, the stability, and the split could be worked out.

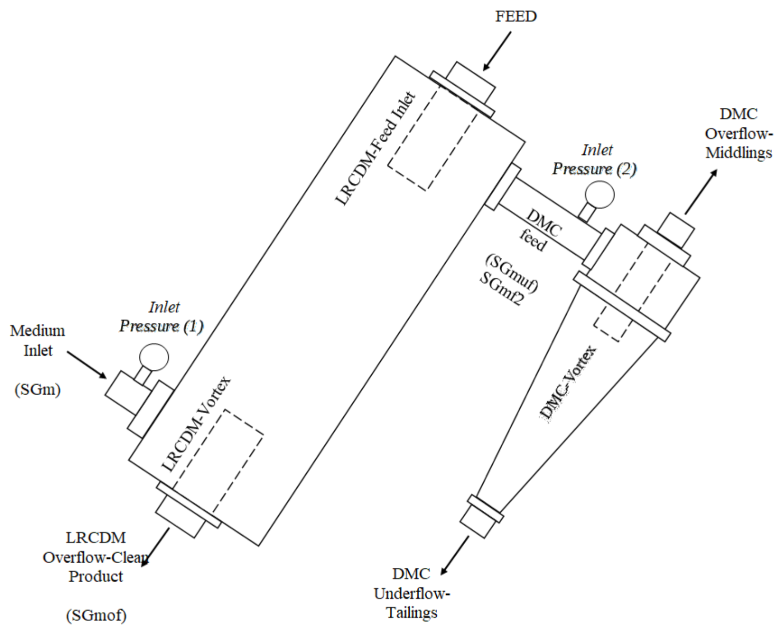

Fig. 1. Layout of the gravity fed three product cyclone, showing the LARCODEM primary separator, the DMC secondary separator, the medium and feed inlets, the product streams, and the adjustable depths and pressures

2.2. Density tracer measurements and calculations

Because separation density depends on particle size, coal was replaced by plastic density tracer cubes (Fig. 2), which allow fast and repeatable readings. The tracers were supplied by Partition Enterprises and DG Lab Services and were used in three sizes of 16, 8, and 4 mm. They covered the density range 1.30 to 2.00 g/cm^3, with 20 tracers in each density class. The 16 mm set rose in steps of 0.10 g/cm^3, while the 8 and 4 mm sets rose in steps of 0.05 g/cm^3. After the circuit reached steady state, all tracers were added at the feed inlet, collected from the drain and rinse screens of each product after about five minutes, and counted. Tracers that stayed inside the unit because of surging were recorded but excluded from the partition calculation. Over the whole programme 12960 tracers were fed and 388 of them, or 3.0%, were not recovered within the collection period. The loss was 5 of 2880 at 16 mm, 78 of 5040 at 8 mm, and 305 of 5040 at 4 mm, that is 0.2, 1.5, and 6.1%. It was concentrated at the finest size and at densities close to the cut point, where the partition curve is flattest and least sensitive to a small loss of counts, so the effect on the reported cut points is small. The probable error at 4 mm may nevertheless be slightly optimistic, and this is stated here so that the 4 mm values are read with that in mind.

Fig. 2. Plastic density tracer cubes used to construct the partition curves. Each density class has its own colour, and 20 cubes per class were fed in each test

Three quantities are used throughout and are kept distinct. The separation density of a stage, also called its cut point and written d_{50}, is the tracer density that divides equally between the two products of that stage. The secondary separation density is the cut point of the DMC stage. The density shift is the difference between the cut point of a stage and the density of the medium that feeds that stage, so it measures how far the cut point sits from its own feed medium rather than from the circulating density set by the operator.

For each stream, the recovery of tracers was plotted against tracer density and fitted to the Whiten partition function by least squares (Napier-Munn et al., 1996):

$$Y = \frac{e^{\alpha x}}{e^{\alpha x} + e^{\alpha} - 2} \quad x = \frac{d}{d_{50}} \tag{1}$$

where d is the tracer density, d_{50} is the cut point, α is the sharpness coefficient, and Y is the partition to the heavy product; the recovery to the overflow shown in Fig. 3 is 100(1 − Y)%. From the fitted curve, the densities d_{25} and d_{75}, at which 25 and 75% report to the heavy product, were read, and the probable error, a measure of the spread of the curve, was calculated as (Wills and Finch, 2016):

$$Ep = (d_{75} - d_{25})/2 \tag{2}$$

The medium stability of a stage, a measure of magnetite segregation, was taken as the density difference between its underflow and overflow medium (Luttrell et al., 2005):

$$Stability = \rho_u - \rho_o \tag{3}$$

where ρ_u and ρ_o are the underflow and overflow medium densities. The medium split was taken as the fraction of the feed medium that leaves through the overflow, and was obtained from the feed, overflow, and underflow medium densities; a value above two-thirds is wanted. The density shift, which measures how far the cut point of a stage sits from the medium that feeds that stage, was defined as:

$$\Delta d_{50} = d_{50} - \rho_f \quad (4)$$

where ρ_f is the feed medium density of the stage. A density shift near zero means the cut point sits at the medium density, which is the most predictable condition.

2.3. Experimental design and modelling

Five variables were studied and are listed in Table 1: the LARCODEM vortex finder depth, the LARCODEM feed pipe immersion depth, the DMC vortex finder depth, the feed pressure, and the medium density. A Taguchi L18 orthogonal array built in Minitab (Taguchi, 1986) reduced the work to 18 conditions. The array carries one factor at two levels and up to seven factors at three levels, and its first five columns were used here, so the medium density was run at two levels and the four geometric and operating variables at three. The geometric and operating variables were coded as minus one, zero, and plus one at their low, centre and high level, and the medium density as minus one and plus one. The magnetite size was held the same throughout. For each response, a second-order model was fitted by least squares (Montgomery, 2017):

$$\hat{Y} = \beta_0 + \Sigma\, \beta_i X_i + \Sigma\, \beta_{ii} {X_i}^2 + \Sigma\, \beta_{ij} X_i X_j \quad (5)$$

where $\hat{Y}$ is the predicted response, the X_i are the coded variables, β_0 is the constant, and the remaining coefficients are the linear, quadratic, and two-factor interaction terms. Terms with probability values above 0.10 were removed step by step, keeping the parent terms of any retained quadratic or interaction terms in the model. Each model was judged by its coefficient of determination R^2, its adjusted $R^{2,}$ and the probability value of the model as a whole. The models are written in coded variables, with the feed pressure coded from the LARCODEM inlet pressure recorded during each run.

Table 1. Independent variables and coded levels

Symbol	Variable	Low	Centre	High
X_1	LARCODEM vortex finder depth (cm)	11	14	17
X_2	LARCODEM feed pipe immersion depth (cm)	8	11	14
X_3	DMC vortex finder depth (cm)	5	10	15
X_4	Feed pressure (inlet head)	6.0	6.5	7.0
X_5	Medium density (g/cm^3)	1.40	*	1.50

* The L18 array carries one factor at two levels, and the medium density was assigned to that column, so it has no centre level.

3. Results and discussion

3.1. Partition behaviour and separation efficiency

Fig. 3 shows the partition curves of both stages for a representative run (Experiment 14). The measured tracer recoveries (symbols) closely follow the fitted Whiten curves (lines). The LARCODEM curves are steep at all three tracer sizes, indicating sharp separation, while the DMC curves are more spread out, especially at 4 and 8 mm. A few DMC tracers near 1.45 to 1.55 g/cm^3 (ringed in Fig. 3b) fell well below the trend through retention and surging in the cyclone body and were left out of the fits, an effect that would repay closer study. The same pattern holds across the whole programme. The primary stage gave a clean and steady separation: its probable error stayed between 0.010 and 0.050 g/cm^3 for every tracer size across all runs. The secondary stage was less even, with the probable error rising from a range of 0.003 to 0.109 g/cm^3 at 16 mm to between 0.007 and 0.151 g/cm^3 at 4 mm. Fig. 4 compares the mean probable error of the two stages at each tracer size. The primary stage stayed between 0.019 and 0.030 g/cm^3 at all three sizes, while the secondary stage rose from 0.016 g/cm^3 at 16 mm to 0.068 g/cm^3 at 8 mm and 0.085 g/cm^3 at 4 mm, so it is far more sensitive to tracer size.

Table 2. Experimental conditions for the 18 runs

Run	Medium density (g/cm³)	Feed pressure	LARCODEM vortex	LARCODEM feed pipe	DMC vortex
1	1.50	6.0	14	8	5
2	1.50	6.0	14	8	15
3	1.50	6.0	11	14	15
4	1.50	6.5	11	14	10
5	1.50	6.5	17	11	10
6	1.50	6.5	17	11	5
7	1.50	7.0	17	8	10
8	1.50	7.0	11	8	15
9	1.50	7.0	14	14	5
10	1.40	7.0	17	14	5
11	1.40	6.0	17	8	15
12	1.40	6.0	17	14	15
13	1.40	6.5	14	11	15
14	1.40	6.5	14	11	10
15	1.40	6.5	14	14	10
16	1.40	7.0	11	8	10
17	1.40	6.0	11	8	5
18	1.40	7.0	11	8	5

Feed pressure as inlet head; all depths in cm. Run 14 is the example shown in Fig. 3.

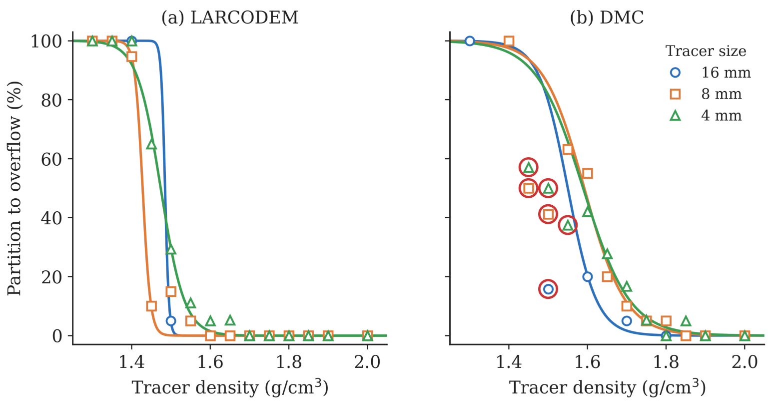

Fig. 3. Partition curves of the (a) LARCODEM and (b) DMC stages for Experiment 14. Symbols are measured tracer recoveries, and lines are the fitted Whiten curves for the 16, 8, and 4 mm tracers

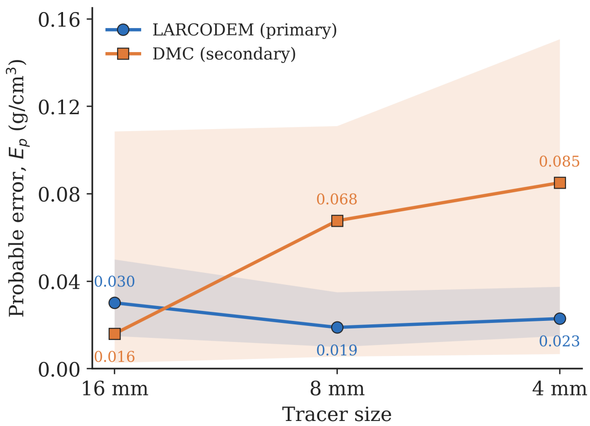

Fig. 4. Mean probable error of the primary (LARCODEM) and secondary (DMC) stages at the three tracer sizes. The secondary stage loses efficiency as the tracer size falls. Shaded bands are the range across the 18 runs

The loss of efficiency at smaller tracer sizes follows the breakaway-size idea: below a size that depends on the cyclone diameter, the centrifugal force on a particle is too small for clean separation, and medium instability strengthens the effect (He and Laskowski, 1995). The primary unit, being wider and fed first, maintained its fine-particle performance, while the narrower secondary unit lost ground at 4 mm.

3.2. Medium stability and its effect on efficiency

Secondary medium stability, defined as the density difference between the secondary underflow and overflow, ranged from 0.095 to 0.427 g/cm³. Most runs sat inside the recommended band of 0.10 to 0.40 g/cm³, as Fig. 5 shows; only Experiment 8 rose above the upper limit. Medium stability and separation efficiency moved together (Fig. 6): as the stability increased, the secondary probable error tended to increase as well, and Experiment 8, the run above the 0.40 limit, also showed a surge. This agrees with the known chain linking a wide medium difference to particle retention and then to poorer separation (Scott et al., 1987; Luttrell et al., 2005).

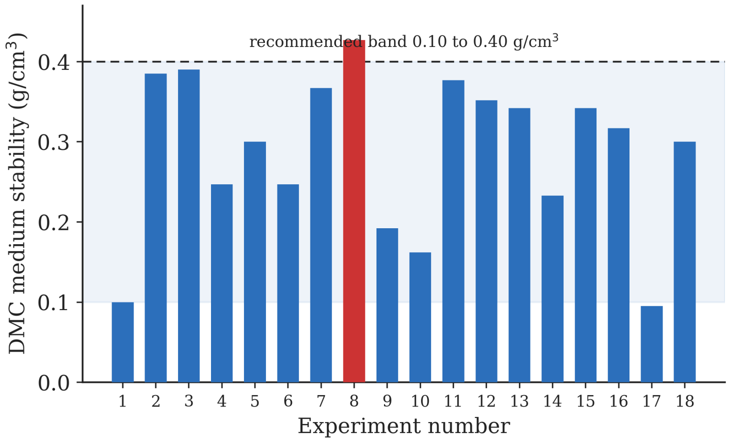

Fig. 5. Secondary stage medium stability for the 18 experiments. The shaded band is the recommended range of 0.10 to 0.40 g/cm³; Experiment 8 (red) is the only run above the limit

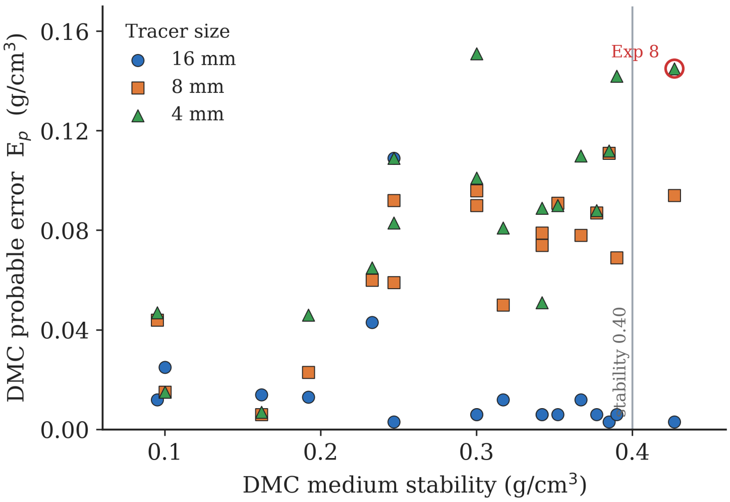

Fig. 6. Secondary stage probable error against medium stability for the three tracer sizes. The error rises with stability, most strongly at the finer sizes; Experiment 8 (circled) is the only run above the limit

The second-order model described medium stability well, with a coefficient of determination of 89.7% and an adjusted value of 84.1% (Table 3). The significant terms were the secondary vortex finder depth ($p < 0.001$), the feed pressure ($p = 0.005$), and their interaction, showing that the same variables that set the secondary medium condition also drive separation efficiency through stability.

3.3. Controlling the secondary separation density

In the three-product unit, the DMC receives a medium that is already denser than the set circulating density, because the LARCODEM sends coarser magnetite to its underflow; the secondary separation density is therefore higher than the set density. How strongly this happens is governed first by the LARCODEM feed pipe immersion depth, which sets the degree of magnetite segregation, a reading supported by the stability model above and by the reported separation density trend (Table 3).

A second-order model captured the secondary density shift well for the two finer tracer sizes. For the 4 mm tracer, the fitted model in coded variables was;

$$\Delta d_{50} = -0.046 + 0.011X_1 - 0.071X_2 + 0.010X_3 + 0.042X_4 + 0.032X_5 + \\ + 0.038X_1X_3 - 0.073X_1X_4 + 0.053X_4X_5 \quad (6)$$

where X_1 to X_5 are the coded variables of Table 1. The model achieved a coefficient of determination of 90.9%, an adjusted value of 82.8%, and Fig. 7 shows that the predicted values lie close to the measured ones. The feed pipe immersion depth was the leading term ($p < 0.001$), followed by the feed pressure and its interaction with the LARCODEM vortex finder depth. The same lead holds at the other two sizes, with the feed pipe immersion depth significant at 8 mm ($p = 0.005$) and at 16 mm ($p = 0.039$), and its coefficient growing as the tracer size falls, from −0.028 at 16 mm to −0.042 at 8 mm and −0.071 at 4 mm (Table 3). The 16 mm model was the weakest of the three at 62.8%, in line with the retention and surging noted for the coarsest tracers in Section 3.1.

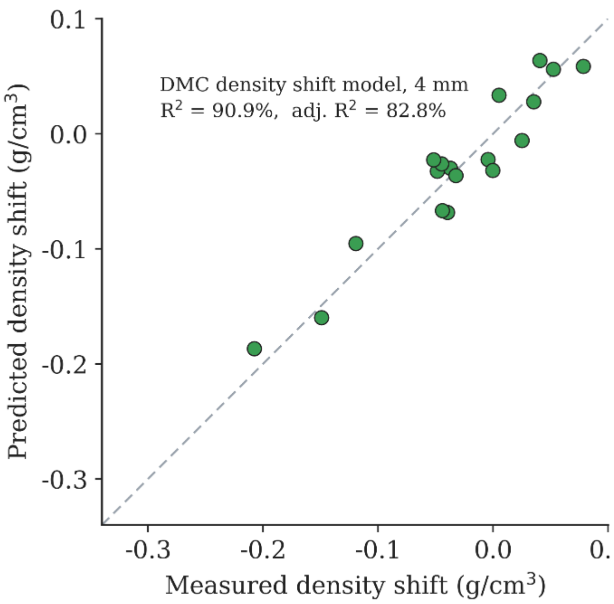

Fig. 7. Predicted against measured DMC density shift for the fitted second-order model (4 mm tracer). The dashed line is the line of equality

Fig. 8 maps the predicted density shift over the feed pipe immersion depth and the recorded inlet pressure, at each of the two circulating densities, with both vortex finder depths held at their centre level. Deepening the feed pipe drives the shift more negative at both densities, so the secondary cut point moves further below the medium that feeds it, while a shallower setting brings the two back together. The map therefore shows the operator which combinations keep the secondary cut point predictable.

The models for the absolute secondary cut point were the strongest of the set, with coefficients of determination of 84.7 to 93.2%, but what they mainly describe is the circulating density itself, which enters every one of them as the leading term ($p < 0.001$), together with the secondary vortex finder depth. That is expected, since the cut point of a stage must follow the density of the medium in the circuit. The density shift is the quantity that isolates what remains once the circulating density is accounted for, and it is there that the feed pipe immersion depth acts. Read together, the two sets of models show that the secondary separation density is not fixed by nature: it can be moved and kept predictable through the feed pipe immersion depth and the feed pressure, independently of the circulating density that the operator has already chosen for the primary stage.

Two points follow for practice. The mechanism is the classification of the magnetite itself, so it belongs to the separator and to the medium rather than to the material being washed, which is why density tracers rather than coal were used here; the coefficients above are specific to this unit, this magnetite, and this density range. Because the feed pipe immersion depth and feed pressure are mechanical settings on the existing unit, the middlings cut can be reset without changing the circulating density, without additional equipment, and without extra consumables.

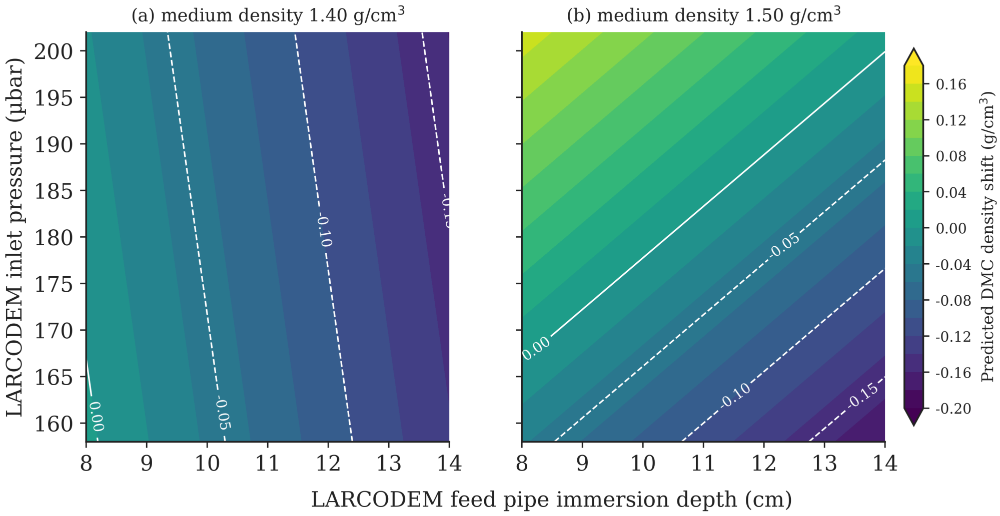

Fig. 8. Predicted DMC density shift as a function of the LARCODEM feed pipe immersion depth and the recorded LARCODEM inlet pressure, at (a) 1.40 and (b) 1.50 g/cm³ circulating density, with both vortex finder depths at their centre level

Table 3. Second-order model summary for the secondary (DMC) stage responses

Response	**Fitted second-order model (coded variables)**	R^2 (%)	**adj.** R^2 (%)	**Model** p
Density shift, 16 mm	$\Delta d_{50} = -0.157 - 0.015X_1 - 0.028X_2 - 0.015X_3 - 0.037X_4 - 0.033X_1X_3$	62.8	47.3	0.022
Density shift, 8 mm	$\Delta d_{50} = -0.076 + 0.022X_1 - 0.042X_2 + 0.046X_3 + 0.020X_4 + 0.027X_5 + 0.063X_4^2 - 0.040X_1X_4 + 0.023X_3X_5$	89.5	80.2	0.001
Density shift, 4 mm	$\Delta d_{50} = -0.046 + 0.011X_1 - 0.071X_2 + 0.010X_3 + 0.042X_4 + 0.032X_5 + 0.038X_1X_3 - 0.073X_1X_4 + 0.053X_4X_5$	90.9	82.8	<0.001
Medium stability	$S = 0.287 + 0.004X_1 + 0.115X_3 + 0.048X_4 + 0.007X_5 + 0.033X_1X_5 - 0.036X_3X_4$	89.7	84.1	<0.001
Separation density, 16 mm	$d_{50} = 1.560 - 0.030X_1 + 0.018X_2 + 0.015X_3 - 0.051X_4 + 0.081X_5 + 0.065X_1X_4 - 0.046X_2X_4 + 0.043X_3X_5$	89.1	79.4	0.002
Separation density, 8 mm	$d_{50} = 1.721 - 0.010X_2 + 0.074X_3 + 0.017X_4 + 0.094X_5 - 0.066X_2^2 - 0.049X_2X_4 + 0.063X_3X_5$	93.2	88.5	<0.001
Separation density, 4 mm	$d_{50} = 1.628 - 0.033X_1 + 0.069X_3 + 0.080X_5 + 0.061X_1^2 + 0.046X_1X_5$	84.7	78.3	<0.001

4. Conclusions

This study provides the first measured evidence that the secondary separation density of a gravity-fed three-product dense medium cyclone can be set intentionally rather than left to develop on its own.

Across the 18 designed runs, the feed pipe immersion depth of the primary unit was the main control: deepening it raised the secondary cut point by enriching the secondary feed in fine magnetite, while shallowing it moved the secondary cut point back toward the set circulating density. Feed pressure and the secondary vortex finder depth also affected the result. Second-order models described the density shift and medium stability of the secondary stage, with coefficients of determination from 63 to 91%. The absolute secondary cut point was modelled well too, from 85 to 93%, but mainly by the circulating density itself. Hence, the density shift remains the quantity through which the secondary cut point is controlled. The primary stage stayed sharp throughout, with a probable error of 0.050 g/cm^3 or less. In contrast, the secondary stage lost efficiency at the finest tracer size and at high medium stability, in line with the breakaway size and surging mechanisms. In practice, the operator can move the secondary cut point and keep it predictable by adjusting feed pipe immersion depth and feed pressure, while monitoring medium stability to keep it within the 0.10 to 0.40 g/cm^3 band.

Acknowledgements

This work was supported by the Istanbul Technical University Scientific Research Projects Coordination Unit (ITU BAP, Project No. MGA-2019-41890). The authors thank KARBOMET Ltd. for providing and modifying the pilot unit. A part of the results reported in this paper were presented at XX Balkan Mineral Processing Congress BMPC 2026 entitled "Second-stage separation density control in a gravity-fed three-product dense medium cyclone".

References

BOSMAN, J., 2014. *The art and science of dense medium selection*. Journal of the Southern African Institute of Mining and Metallurgy 114, 529-536.

COLLINS, D.N., TURNBULL, T., WRIGHT, R., NGAN, W., 1983. *Separation efficiency in dense medium cyclones*. Transactions of the Institution of Mining and Metallurgy 92, 38-51.

DAVIS, J.J., NAPIER-MUNN, T.J., 1987. *The influence of medium viscosity on the performance of dense medium cyclones in coal preparation*. Proceedings of the 3rd International Conference on Hydrocyclones, Oxford.

FOURIE, P.J., VAN DER WALT, P.J., FALCON, L.M., 1980. *Beneficiation of fine coal by dense medium cyclone*. Journal of the South African Institute of Mining and Metallurgy 80, 357-361.

HE, Y.B., LASKOWSKI, J.S., 1995. *Dense medium cyclone separation of fine particles*. Coal Preparation 16, 1-49.

JACOBS, J., DE KORTE, G.J., 2013. The three product cyclone: adding value to South African coal processing. Journal of the Southern African Institute of Mining and Metallurgy 113, 859-863.

KING, R.P., JUCKES, A.H., 1984. *Cleaning of fine coals by dense medium hydrocyclone*. Powder Technology 40, 147-160.

LUTTRELL, G.H., BARBEE, C.J., BETHELL, P.J., WOOD, C.J., 2005. *Dense medium cyclone optimization*. Final Technical Report, U.S. Department of Energy.

MONTGOMERY, D.C., 2017. *Design and Analysis of Experiments*, 9th ed. Wiley, Hoboken.

NAPIER-MUNN, T.J., 1990. *The effect of dense medium viscosity on separation efficiency*. Coal Preparation 8, 145-165.

NAPIER-MUNN, T.J., MORRELL, S., MORRISON, R.D., KOJOVIC, T., 1996. Mineral Comminution Circuits: Their Operation and Optimisation. JKMRC, Brisbane.

O'BRIEN, M., FIRTH, B., McNALLY, C., 2014. *Effect of medium composition on dense medium cyclone operation*. International Journal of Coal Preparation and Utilization 34, 121-132.

PURAL, Y.E., SIRKECI, A.A., BOYLU, F., 2023. *Simulation and performance evaluation of three product dense medium cyclone*. International Journal of Coal Preparation and Utilization 43, 1299-1312.

SCOTT, I., BAGULEY, P., NAPIER-MUNN, T., 1987. *The influence of medium rheology on the separation of minerals in dense medium drums and cyclones*. Proceedings of the Dense Medium Operators Conference, AusIMM, 205-233.

SHAH, C.L., 1992. *LARCODEM separator: development of three product unit*. In Innovations in Physical Separation Technologies, Springer Netherlands, 263-274.

TAGUCHI, G., 1986. *Introduction to Quality Engineering*. Asian Productivity Organization, Tokyo.

WILLS, B.A., FINCH, J.A., 2016. *Wills' Mineral Processing Technology*, 8th ed. Butterworth-Heinemann, Boston.

XIA, Y., FEI, Y., ZHAO, S., 2013. *Washing study of high ash Indian coal with three product heavy medium cyclone process*. XVII International Coal Preparation Congress, Ankara, 271-276.